Performance Trade-off Analysis of ISAC Systems Using Kullback-Leibler Divergence

Mohammad A. Al-Jarrah†, Emad Alsusa†, Yousef Kloob†, and Christos Masouros‡
† School of Electrical and Electronic Engineering,
The University of Manchester, Manchester, M13 9PL, UK
email:{mohammad.al-jarrah, e.alsusa, yousef.kloob}@manchester.ac.uk.
‡ University College London, email: c.masouros@ucl.ac.uk.

***Abstract*—This paper delves into the achievable trade-off in the performance of sensing and communication subsystems in integrated sensing and communication (ISAC) setup using the Kullback-Leibler divergence (KLD) as an information-theoretical tool. The system model under consideration consists of a multiple-input-multiple-output (MIMO) base-station (BS) that simultaneously serves communication user equipments (CUEs) and detects targets using the same resources. The KLD framework offers a unified performance measure that encapsulates both the error rate of CUEs and the detection capability of targets. Moreover, the interrelationship between target detection capability, CUE error rate, and the proposed KLD is thoroughly investigated and elucidated. Theoretical derivations, corroborated by simulations, validate the high accuracy of the derived KLD in characterizing the performance of both subsystems. The findings of this study facilitate a holistic design of ISAC systems for next-generation wireless networks by providing insights into the sensing-communication performance trade-off.**

***Index Terms*—Kullback-Leibler divergence, integrated sensing and communication (ISAC), MIMO radar, precoding.**

I. Introduction

THE integration between radar and communication systems has been introduced as a promising paradigm, known as integrated sensing and communication (ISAC), which allows for efficient utilization of base-station (BS) resources for concurrent sensing and communication services [1]. ISAC systems have garnered substantial attention from both academic and industrial researchers, with major companies like NOKIA, SAMSUNG, and HUAWEI recognizing their importance for the forthcoming 6G networks [4]–[6]. The allocation of spectral and hardware resources for joint sensing and communication purposes has become a focal point in the development of future wireless networks.

ISAC systems find applications in diverse domains, ranging from sensing-assisted communication [2], [3], to innovative technologies like internet-of-things (IoT) massive connectivity, and ground and aerial autonomous vehicles. The seamless integration of sensing and communication capabilities in these systems has the potential to revolutionize various facets of wireless networks by enabling enhanced situational awareness, improved resource utilization, and support for novel use cases.

Given the anticipated widespread deployment of ISAC systems in 6G networks, it is crucial to investigate their feasibility, performance trade-offs, and develop efficient signaling and data processing techniques. Existing literature has examined the performance analysis of ISAC systems from different perspectives. For instance, [7] considered the communication user's rate and radar detection probability, while [8] and [9] explored uplink and downlink data transmissions in ISAC systems. The achievable ergodic capacity, outage probability, and diversity order have been analyzed for communication users, and the sensing rate has been used to assess the radar system. Furthermore, [10] and [11] studied the detection probability for the radar sensing component and the spectral efficiency of the communication part in an ISAC setting.

Nevertheless, the trade-off between sensing and communication performance is typically investigated using different performance evaluation measures. For instance, the bit error rate is usually employed for communication subsystem whereas the detection probability is applied for the sensing subsystem. Introducing the Kullback-Leibler divergence (KLD) as a unified measure that encompasses both systems could significantly benefit the analysis and optimization of ISAC systems [13], [14]. Moreover, a low-complexity unified objective function utilizing the KLD measure would facilitate the optimization of available network resources [15]. The development of a holistic framework for evaluating and optimizing the performance of ISAC systems is essential for their practical deployment and operation.

This paper explores the trade-off between communication and sensing performance by employing the KLD as a unified performance measure applicable to both subsystems. We demonstrate that KLD effectively captures the detection performance for both systems by establishing its relationship with the symbol error rate (SER) of the communication part and the probability detection for of the radar subsystem. The obtained results confirm the accuracy of our derivations and showcase the informative nature of the proposed KLD in characterizing ISAC holistically.

The remainder of this paper is organized as follows. Sec. II explains the considered system. In Secs. III and IV,

the trade-off analysis using KLD is presented for both the communication and radar parts, respectively. The numberical results are introduced in Sec. V, and finally, conclusions are drawn in Sec. VI.

II. System Model

As shown in Fig. 1, the considered system model consists of N antenna MIMO BS serving a number of K communication user equipments (CUEs) by streaming data in downlink, and aiming at detecting the possible existence of an unmanned aerial vehicle (UAV). The BS exploits the whole antenna array and resource block for both simultaneous functionalities. This kind of ISAC setup is typically referred in the literature as the shared deployment. The BS applies the widely accepted zero forcing (ZF) as a simple and practical method for precoding the CUEs information symbols that are denoted as $\mathbf{d_w}$ [16]. The radar waveform matrix $\mathbf{S} = [\mathbf{s}_1, \mathbf{s}_2, \cdots, \mathbf{s}_L]$ with L represents the number of snapshots and $\mathbf{s}_l \in \mathbb{C}^{N\times 1}$ is the signals vector in snapshot l, is designed at the BS such that the resulting covariance matrix $\mathbf{R}_s \triangleq \frac{1}{L}\sum_{l=1}^{L} \mathbf{s}_l\mathbf{s}_l^H$ fulfills a desired form, for example, $\mathbf{R}_s = \mathbf{I}_N$ is used for omnidirectional MIMO radar. Thereafter, a linear combiner is used to superimpose both the radar and precoded communication signals to form the equivalent integrated waveform vector that is emitted by the BS's antenna array. The available power resources at the BS, P_T, is also divided over the radar and communication subsystems with P_{com} and $P_{\text{rad}} = P_T - P_{\text{com}}$, respectively. The integrated ISAC signal can be written as

$$\tilde{\mathbf{d}}_{\text{ISAC}}[l] = \sqrt{P_{\text{com}}}\mathbf{d_w}[l] + \sqrt{P_{\text{rad}}}\mathbf{s}_l \tag{1}$$

For transmission interval l, a data symbol $d_k[l]$ intended for the kth CUE is taken from M-ary phase shift keying (MPSK) constellation, and precoded using a ZF with a precoding vector $\mathbf{w}_k \in \mathbb{C}^{N\times 1}$. Using ZF precoding, the precoding matrix $\mathbf{W} \in \mathbb{C}^{N\times K} = [\mathbf{w}_1, \mathbf{w}_2, \cdots, \mathbf{w}_K]$ can be generally formulated in a closed form as $\mathbf{W} = \mathbf{G}^*\left(\mathbf{G}^T\mathbf{G}^*\right)^{-1}$, where $\mathbf{P} \in \mathbb{C}^{K\times K}$ is a diagonal matrix that is used to prioritize users by controlling the transmit power of CUEs, and $\mathbf{G} \in \mathbb{C}^{N\times K} = [\mathbf{g}_1, \mathbf{g}_2, \cdots, \mathbf{g}_K]$ is the channel matrix of all users to the N-antenna BS. In this paper, we consider the flat Rayleigh fading channel model with independent identically distributed channels (iid). Accordingly, the baseband received signals at CUEs can be written as [14]

$$\mathbf{y}[l] = \mathbf{P}\mathbf{d} + \eta \tag{2}$$

The matrix $\mathbf{P}$ can be expressed as $\mathbf{P} \triangleq \alpha_{\text{ZF}}\mathbf{P}_{\text{com}} = \sqrt{N-K+1}\mathbf{P}_{\text{com}}$, where $\alpha_{\text{ZF}} = \sqrt{N-K+1}$ is used to fix the transmit power, and $\mathbf{P}_{\text{com}} \triangleq \text{diag}\left(\sqrt{P_{1,\text{com}}}, \sqrt{P_{2,\text{com}}}, \cdots, \sqrt{P_{K,\text{com}}}\right)$ is used to control the portion of transmission power intended for the direction of each of the CUEs. The total amount of power for the communication subsystem is limited to P_{com}, thus we have $\sum_k P_{k,\text{com}} = P_{\text{com}}$. For uniform power distribution among CUEs, $P_{k,\text{com}}$ can be chosen such that

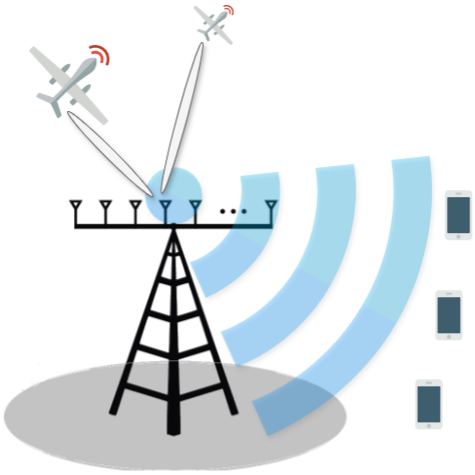

a) An example of ISAC system with 3 CUEs and 2 targets.

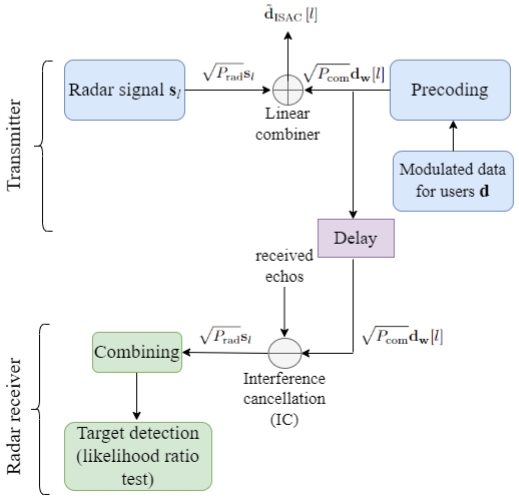

b) Block diagram for the transmitter at the BS, and receiving radar subsystem at the BS.

Fig. 1. An ISAC system setup with 3 CUEs and 2 targets.

$P_{k,\text{com}} = \frac{P_{\text{com}}}{K}$. Accordingly, the received signal at user k corrupted by radar interference and noise can be written as

$$y_k[l] = \sqrt{P_{k,\text{com}}}\alpha_{\text{ZF}}d_k[l] + \eta_k \tag{3}$$

where $\eta_k \triangleq \sqrt{P_{\text{rad}}}\mathbf{g}_k^T\mathbf{s}_l + n_k$ is a noisy term that accounts for the radar interference plus additive white Gaussian noise (AWGN) with each element in the vector $\mathbf{g}_k^T \in \mathbb{C}^{N\times 1}$ is $\mathcal{CN}\left(0, 2\sigma_g^2\right)$ is a flat Rayleigh fading factor and $n_k \sim \mathcal{CN}\left(0, 2\sigma_n^2\right)$ is the AWGN. It can be shown that $\eta_k \sim \mathcal{CN}\left(0, 2\sigma_\eta^2\right)$ where $\sigma_\eta^2 = P_{\text{rad}}\sigma_g^2 + \sigma_n^2$.

The radar waveform vector $\mathbf{s}_l \in \mathbb{C}^{N\times 1} \forall l \leq L$ is transmitted during the time period l. This signal is emitted towards a certain direction to test the possible existence of a potential target in that direction. In the case of target existence, the signal gets reflected by the target and the BS will receive echo in the reception phase. Now, let $\mathbf{a}_{\text{T}}(\theta)$ and $\mathbf{a}_{\text{R}}(\theta)$ denote the array manifolds of a uniform

linear array (ULA) in the transmission and reception phases, respectively. Accordingly, by using the well-known binary hypothesis testing problem formulation, the received signals vector at the BS antennas can be expressed as

$$\tilde{\mathbf{y}}_{\mathrm{rad}}[l]=\begin{cases} H_1{:}\alpha_t\sqrt{P_{\mathrm{rad}}}\mathbf{a}_{\mathrm{R}}(\theta)\,\mathbf{a}_{\mathrm{T}}(\theta)^T\mathbf{s}_l \\ \qquad +\sqrt{P_{\mathrm{com}}}\mathbf{G}_{\mathrm{rad}}\mathbf{d}_{\mathbf{w}}[l]+\mathbf{n}_{\mathrm{rad}}[l] \\ H_0{:}\sqrt{P_{\mathrm{com}}}\mathbf{G}_{\mathrm{rad}}\mathbf{d}_{\mathbf{w}}[l]+\mathbf{n}_{\mathrm{rad}}[l] \end{cases} \tag{4}$$

where H_1 and H_0 respectively represent the presence and absence of a target in the direction of interest θ, α is a factor that represents the gain of the signal path BS-Target-BS, the term $\sqrt{P_{\mathrm{rad}}}\mathbf{G}_{\mathrm{rad}}\mathbf{d}_{\mathbf{w}}[l]$ represents the interference resulted from the communication signal, $\mathbf{G}_{\mathrm{rad}}^T \in \mathbb{C}^{N\times N}$ is the interference or clutter channel matrix, and $\mathbf{n}_{\mathrm{rad}} \in \mathbb{C}^{N\times 1} \sim \mathcal{CN}\left(0, 2\sigma_n^2\mathbf{I}_N\right)$ is the AWGN vector with $\mathbf{I}_N$ is the identity matrix. We assume that the channel state information (CSI) of $\mathbf{G}_{\mathrm{rad}}$ is estimated at the BS in a previous stage, and thus since the BS has knowledge about the data it has sent, i.e., $\sqrt{P_{\mathrm{rad}}}\mathbf{d}_{\mathbf{w}}[l]$, using interface cancellation (IC) approach is very beneficial to subtract $\mathbf{G}_{\mathrm{rad}}\mathbf{d}_{\mathbf{w}}[l]$ from the received signals vector $\tilde{\mathbf{y}}_{\mathrm{rad}}[l]$. It is noteworthy highlighting that $\mathbf{G}_{\mathrm{rad}}$ estimates can be found at the BS in a previous phase by transmitting a communication signal only and measuring the received echo accordingly. Nevertheless, given imperfectly estimated channel matrix $\hat{\mathbf{G}}_{\mathrm{rad}}$, and by employing the imperfect IC procedure described above, the received signals vector in (4) can be re-expressed as

$$\mathbf{y}_{\mathrm{rad}}[l] = \begin{cases} H_1 : \alpha_t\sqrt{P_{\mathrm{rad}}}\mathbf{A}(\theta)\,\mathbf{s}_l + \omega_{\mathrm{rad}} + \mathbf{n}_{\mathrm{rad}}[l] \\ H_0 : \omega_{\mathrm{rad}} + \mathbf{n}_{\mathrm{rad}}[l] \end{cases} \tag{5}$$

where $\mathbf{A}(\theta) = \mathbf{a}_{\mathrm{R}}(\theta)\times\mathbf{a}_{\mathrm{T}}$ is the equivalent array manifold, and $\omega_{\mathrm{rad}} \in \mathbb{C}^{N\times 1} = \mathbf{G}_{\mathrm{err}}^T\mathbf{d}_{\mathbf{w}}[l] = \mathbf{G}_{\mathrm{err}}^T\sum_{i=1}^{K}\sqrt{p_k}\mathbf{w}_k d_k[l]$ is remaining residual interference after applying IC. Here, $\mathbf{G}_{\mathrm{err}} \triangleq \mathbf{G}_{\mathrm{rad}} - \hat{\mathbf{G}}_{\mathrm{rad}}$ denotes the channel estimation errors. In this work, the estimation errors are characterized using a complex Gaussian random variable with a mean of 0 and a variance of σ_{err}^2.

Since the same array, i.e., the BS array, is used for transmitting and receiving echoes from the target, the monostatic radar concept applies with $\mathbf{a}(\theta) \triangleq \mathbf{a}_{\mathrm{R}}(\theta) = \mathbf{a}_{\mathrm{T}}(\theta) \triangleq \left[1, \mathrm{e}^{j\frac{2\pi\Delta}{\lambda_0}\sin(\theta)}, \cdots, \mathrm{e}^{j\frac{2\pi\Delta}{\lambda_0}(N-1)\sin(\theta)}\right]^T$, thus the equivalent array manifold is $\mathbf{A}(\theta) \in \mathbb{C}^{N\times N} = \mathbf{a}(\theta)\,\mathbf{a}(\theta)^T$.

III. The KLD of Communication System

The achievable KLD for the communication subsystem that employs ZF as a precoding scheme at BS will be evaluated. According to the received signal model $y_k[l]$ in (3), the probability density function $f(y_k|d_k[l])$ follows a complex normal distribution, which can be given by

$$f(y_k|d_k[l]) = 1/\left(\sqrt{(2\pi)^2|\Sigma|}\right)\mathrm{e}^{-(\mathbf{y}_k-\mu_k)^T\,\Sigma^{-1}(\mathbf{y}_k-\mu_k)} \tag{6}$$

where $\mathbf{y}_k \triangleq [y_{k,\Re}, y_{k,\Im}]^T$ with $y_{k,\Im} = \Im(y_k)$ and $y_{k,\Re} \triangleq \Re(y_k)$ respectively represent the imaginary part and real part of a complex valued signal y_k, $\mu_k \triangleq [\mu_{k,\Re}, \mu_{k,\Im}]^T$ is the mean vector with $\mu_{k,\Re} = \sqrt{P_{k,\mathrm{com}}}\alpha_{\mathrm{ZF}}\Re(d_k[l])$ and $\mu_{k,\Im} = \sqrt{P_{k,\mathrm{com}}}\alpha_{\mathrm{ZF}}\Im(d_k[l])$, and $\Sigma = \sigma_\eta^2\mathbf{I}_2$ is the covariance matrix Σ. It can be easily shown that the determinant and inverse of the covariance matrix are respectively $|\Sigma| = \sigma_\eta^4$ and $\Sigma^{-1} = \frac{1}{\sigma_\eta^2}\mathbf{I}_2$.

For a certain data symbols constellation, such as MPSK, KLD needs to be computed for every pair of dissimilar data symbols $\{d_{k,n}[l], d_{k,m}[l]\}$, and then the average of all possible pairs is evaluated. Let us denote a pair of dissimilar symbols as $\{d_{k,n}[l], d_{k,m}[l]\}\,\forall n \neq m$, and the conditional density functions of the received signal given $d_{k,n}[l]$ and $d_{k,m}[l]$ by $f_n \sim \mathcal{CN}(\mu_{k,n}, \Sigma_n)$ and $f_m \sim \mathcal{CN}(\mu_{k,n}, \Sigma_m)$, respectively, thus $\mathrm{KLD}_{n\to m}$ can be derived as [14],

$$\begin{aligned}\mathrm{KLD}_{k,n\to m} = \frac{1}{2\ln 2}\Bigg(&\mathrm{tr}\left(\Sigma_m^{-1}\Sigma_n\right) - 2 + \ln\frac{|\Sigma_m|}{|\Sigma_n|} \\ &+ (\mu_{k,m}-\mu_{k,n})^H\Sigma_m^{-1}(\mu_{k,m}-\mu_{k,n})\Bigg)\end{aligned} \tag{7}$$

Moreover, by observing that $\Sigma_m = \Sigma_n = \sigma_\eta^2\mathbf{I}_2$ and $\mu_{k,m} = \left[\sqrt{P_{k,\mathrm{com}}}\alpha_{\mathrm{ZF}}\cos\phi_{k,m}, \sqrt{P_{k,\mathrm{com}}}\alpha_{\mathrm{ZF}}\sin\phi_{k,m}\right]$, $\mathrm{KLD}_{n\to m}$ for ZF based communication subsystem reduces to

$$\begin{aligned}\mathrm{KLD}_{k,n\to m}^{\mathrm{ZF}} &= \frac{1}{2\sigma_\eta^2\ln 2}(\mu_{k,m}-\mu_{k,n})^H(\mu_{k,m}-\mu_{k,n}) \\ &= \frac{\gamma_{k,\mathrm{ZF}}}{\ln 2}(1-\cos(\phi_{k,m}-\phi_{k,n}))\end{aligned} \tag{8}$$

where $\gamma_{k,\mathrm{ZF}} = \frac{\alpha_{\mathrm{ZF}}^2 P_{k,\mathrm{com}}}{\sigma_\eta^2}$.

As mentioned above, since KLD is measured for a pair of PDFs associated with a pair of dissimilar data symbols, the average KLD, $\mathrm{KLD}_{k,\mathrm{avg}}^{\mathrm{ZF}}$, can be simply calculated by taking into account all possible dissimilar pairs of symbols. Therefore, the average KLD can be found by

$$\begin{aligned}\mathrm{KLD}_{k,\mathrm{avg}}^{\mathrm{ZF}} &= \frac{\gamma_{\mathrm{LTZF}}}{\ln 2}\sum_{m=1}^{M}\sum_{\substack{n=1\\n\neq m}}^{M}\Pr(\phi_{k,m},\phi_{k,n}) \\ &\quad\times\ (1-\cos(\phi_{k,m}-\phi_{k,n})) \\ &= \frac{\lambda}{M(M-1)\ln 2}\gamma_{\mathrm{LTZF}}\end{aligned} \tag{9}$$

where $\lambda = \sum_{m=1}^{M}\sum_{\substack{n=1\\n\neq m}}^{M}(1-\cos(\phi_{k,m}-\phi_{k,n}))$. Finally, by considering a multi-user case scenario, the average KLD for all CUEs can be evaluated as

$$\mathrm{KLD}_{\mathrm{ZF}} = \frac{1}{K}\sum_{k=1}^{K}\mathrm{KLD}_{k,\mathrm{avg}}^{\mathrm{ZF}} \tag{10}$$

IV. Radar System Achievable KLD

By using (5) and representing the error resulted from imperfect IC process as a complex Gaussian distributed random variable, i.e., $\omega_{\mathrm{rad}} \sim \mathcal{CN}\left(0, 2\sigma_\omega^2\mathbf{I}_N\right)$, then the received radar signals can be expressed as

$$\mathbf{y}_{\mathrm{rad}}[l] = \begin{cases} H_1 : \alpha_t\sqrt{P_{\mathrm{rad}}}\mathbf{A}(\theta)\,\mathbf{s}_l + \tilde{\omega}_{\mathrm{rad}} \\ H_0 : \tilde{\omega}_{\mathrm{rad}} \end{cases} \tag{11}$$

where $\tilde{\omega}_{\mathrm{rad}} \sim \mathcal{CN}\left(0, 2\sigma_{\tilde{\omega}}^2\mathbf{I}_N\right)$ with $\sigma_{\tilde{\omega}}^2 = \sigma_\omega^2 + \sigma_n^2$ and $\sigma_\omega^2 = \sigma_{\mathrm{err}}^2\sigma_{\mathrm{w}}^2 N\sum_{i=1}^{K}P_{k,\mathrm{com}}$. After receiving the echos

corresponding to the L snapshots, the BS linearly combines the received vectors as

$$\tilde{y}_{\text{rad}} = \frac{1}{L}\sum_{l=1}^{L} \mathbf{s}_l^H \mathbf{y}_{\text{rad}}[l] \tag{12}$$

Consequently, the KLD for the radar system can be evaluated based on (12) as

$$\text{KLD}_{k,H_0\to H_1} = \frac{1}{2\ln 2}\left(\text{tr}\left(\Sigma_{H_1}^{-1}\Sigma_{H_0}\right) - 2 + \ln\frac{|\Sigma_{H_1}|}{|\Sigma_{H_0}|} + \left(\mu_{H_1}-\mu_{H_0}\right)^H \Sigma_{H_1}^{-1}\left(\mu_{H_1}-\mu_{H_0}\right)\right) \tag{13}$$

where $\mu_{H_1} = \alpha_t\sqrt{P_{\text{rad}}}\frac{1}{L}\sum_{l=1}^{L}\mathbf{s}_l^H\mathbf{A}(\theta)\mathbf{s}_l$, $\mu_{H_0}=0$, and $\Sigma_{H_0}=\Sigma_{H_1}=\frac{2}{L^2}\sigma_\omega^2\sum_{l=1}^{L}\sum_{n=1}^{N}|\mathbf{s}_l(n)|^2 = \frac{2}{L^2}\sigma_\omega^2\text{Tr}(\mathbf{R}_s)$. Since $\Sigma_{H_0}=\Sigma_{H_1}$ and they are scalar values, the KLD is symmetric and can be reduced to

$$\begin{aligned}\text{KLD}_{k,H_i\to H_q} &= \frac{1}{2\ln 2}\left(\mu_{H_1}-\mu_{H_0}\right)^H\Sigma_{H_1}^{-1}\left(\mu_{H_1}-\mu_{H_0}\right)\\ &= \frac{1}{4\ln 2}\frac{\alpha_t^2 P_{\text{rad}}}{\sigma_\omega^2\text{Tr}(\mathbf{R}_s)}\left|\text{sum}(\mathbf{R}_s\odot\mathbf{A}(\theta))\right|^2\end{aligned} \tag{14}$$

where $\{i,q\}\in\{0,1\}$, and $\odot$ and $\text{sum}(X)$ respectively indicate the scalar product and the sum of all matrix X elements.

The target detection process is executed by comparing the linearly combined received signal $\tilde{y}_{\text{rad}}$ with a threshold τ using a likelihood ratio test as follows,

$$\tilde{y}_{\text{rad}} \underset{H_0}{\overset{H_1}{\gtrless}} \tau \tag{15}$$

The false alarm and detection probabilities, P_D and P_{FA}, are determined by the distributions of $\tilde{y}_{\text{rad}}$ under H_0 and H_1, respectively, and the choice of the threshold τ. Given that $\tilde{y}_{\text{rad}}$ follows complex Gaussian distributions under both hypotheses, with means μ_{H_0} and μ_{H_1}, and a common variance Σ_{H_1}, the closed-form expressions for P_D and P_{FA} can be derived as,

$$P_D = Q\left(\frac{\tau-\mu_{H_1}}{\sqrt{\Sigma_{H_1}}}\right),\quad P_{FA} = Q\left(\frac{\tau-\mu_{H_0}}{\sqrt{\Sigma_{H_1}}}\right) \tag{16}$$

where $Q(\cdot)$ is the complementary cumulative distribution function (CCDF) of the standard normal distribution.

V. Numerical Results

In this section, we introduce the performance evaluation of the ISAC system that is described in this paper. Monte Carlo method with 10^6 runs for each simulation point is employed here. A use case scenario of a number of two CUEs which use QPSK signalling and a single target is considered with a number of 100 snapshots. A total number of 50 antennas is considered at the BS with half-wavelength separation, $\Delta = 0.5\lambda$. Moreover, the power budget at the BS is set to $P_T = 1$, and the target is positioned at a direction of $\theta = 35^o$. The designed radar covariance matrix satisfies the omnidirectional MIMO radar condition, i.e., $\mathbf{R}_s = \mathbf{I}_N$, and the radar channel pathloss is normalized to unity $\alpha = 1$ to simplify the calculation of SNR. The channel estimation error in $\mathbf{G}_{\text{rad}}$ as described below (5) has a variance of $\sigma_{\text{err}}^2 = 0.01$.

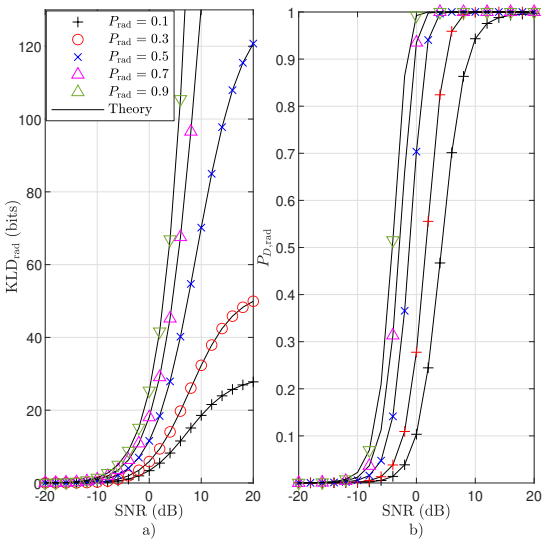

Fig. 2. The performance of the radar subsystem: a) The achievable KLD_{rad}, and b) The detection probability $P_{D,\text{rad}}$.

Fig. 2 shows the achievable performance for the radar subsystem under different allocated radar power ratios. The performance is assessed using the KLD is illustrated in Fig. 2.a. Meanwhile, the detection probability P_D, where the false alarm rate is fixed at 10^{-4}, is shown in Fig. 2.b. The figure demonstrates a perfect agreement between the theoretical KLD derived in this paper and the simulation results. As evident from the figure, there is a direct proportional relationship between the detection capability of the radar subsystem and the KLD, indicating that an increase in KLD corresponds to an improvement in P_D. The figure also showcases the impact of allocated radar power portion P_{rad} on the radar subsystem's performance, with both KLD and P_D exhibiting an upward trend as P_{rad} increases.

In Fig. 3, the performance of the communication subsystem is shown under different values of radar transmit power P_{rad}. The figure clearly demonstrates the inverse relationship between the KLD and the error rate for the communication part. A perfect agreement between the derived and simulated KLD is observed, validating the accuracy of the theoretical analysis. As evident from the figure, increasing P_{rad} significantly degrades the communication performance. For instance, error floors of 0.002 and 0.1 are reached when $P_{\text{rad}} = \{0.7, 0.9\}$, respectively, indicating that further increasing the signal-to-noise ratio (SNR) cannot mitigate this performance degradation. These error floors arise due to the substantial interference from the radar system to the communication subsystem. Moreover, Fig. 3.a reveals a saturation behavior of the KLD at high values of P_{rad}, suggesting a diminishing return in terms of communication performance improvement beyond a certain radar transmit

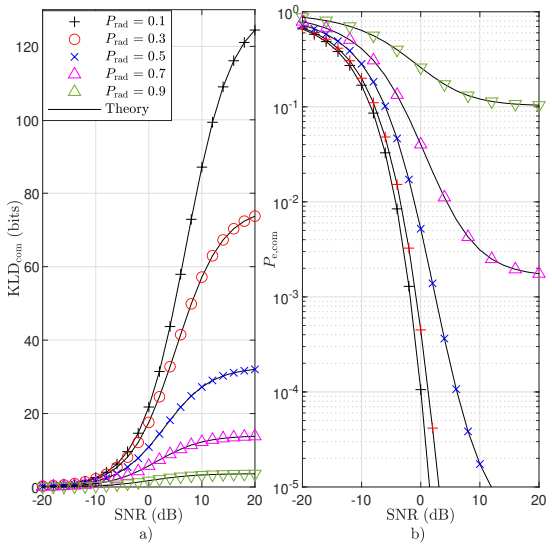

Fig. 3. The performance of the communication subsystem: a) The achievable KLD_{com}, and b) The symbol error rate $P_{\text{e,com}}$.

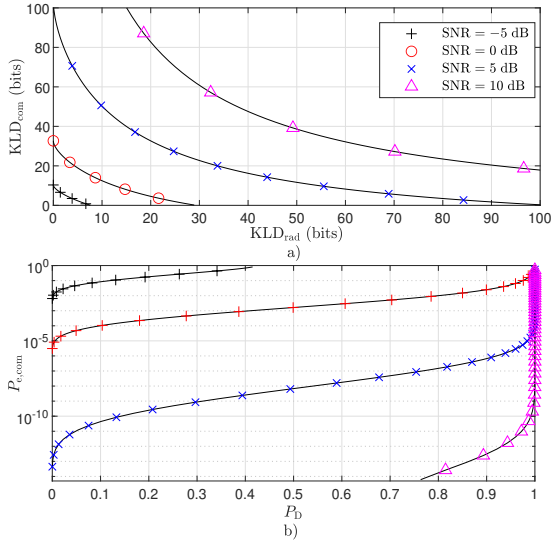

Fig. 4. The trade-off performance of the radar-communication subsystems in an ISAC setup: a) The $\text{KLD}_{\text{rad}} - \text{KLD}_{\text{com}}$, and b) The $P_D - P_{\text{e,com}}$.

power threshold. This observation highlights the critical trade-off between radar and communication in ISAC.

Fig. 4 illustrates the trade-off between communication and radar subsystems using both the KLD-KLD and the P_D-$P_{\text{e,com}}$ trade-offs through analytical solutions. The KLD-based trade-off in Fig. 4.a clearly demonstrates the inherent compromise between the performance of the two subsystems. It is evident that both systems suffer from poor detection capabilities at low SNR values. For instance, when the SNR is 5 dB, the maximum achievable KLD is less than 30 bits, which is attained when the other system's KLD is 0 bits. This observation underscores the challenge of achieving high-performance ISAC at low-SNR.

On the other hand, Fig. 4.b reveals a highly non-linear trade-off between the detection probability P_D and the communication error probability $P_{\text{e,com}}$, particularly at the extreme ends of the considered P_D range. For example, when $P_D > 0.9$, there is a sharp increase in $P_{\text{e,com}}$, indicating a significant degradation in communication performance. Similarly, when $P_D < 0.1$, a rapid performance improvement in communication performance is observed. This sudden change in the trade-off characteristics poses challenges for system design, especially if the desired $P_{\text{e,com}}$ values are extremely low, such as less than 10^{-10}. Dealing with such small probabilities requires large memory and computational resources, further complicating the design process.

VI. Conclusion

This work investigated ISAC with a single MIMO-BS aims at serving multiple CUEs while detecting a target in a certain direction. For the communication subsystem, ZF precoding technique was utilized to multiplex the data symbols of the CUEs. The KLD was derived for the integrated subsystems, i.e., the radar and communication parts, where the impact of interference was taken into account. The accuracy of the derived KLD expressions was validated through Monte Carlo simulations, revealing a fundamental trade-off between the two subsystems. Specifically, enhancing one subsystem's performance leads to a degradation in the other due to power distribution among subsystems and increased interference. The KLD-based trade-off analysis provides a tractable approach for characterizing the performance of ISAC systems, contributing to a deeper understanding of the interplay between sensing and communication functionalities. The results and analysis presented in this paper have important implications for the design and deployment of future wireless networks that integrate sensing and communication capabilities. As the demand for such systems grows, the development of efficient techniques for balancing the performance of both subsystems is essential. The KLD-based framework introduced in this work represents a significant step towards achieving this goal.

References

[1] A. Liu *et al.*, "A survey on fundamental limits of integrated sensing and communication," *IEEE Commun. Surveys Tuts.*, Early access, 2022.

[2] F. Liu *et al.*, "Integrated sensing and communications: Toward dual-functional wireless networks for 6G and beyond," *IEEE J. Sel. Areas Commun.*, vol. 40, no. 6, pp. 1728-1767, Jun. 2022.

[3] M. A. Al-Jarrah, A. Al-Dweik, S. Ikki, and E. Alsusa, "Spectrum-occupancy aware cooperative spectrum sensing using adaptive detection," *IEEE Sys. J.*, vol. 14, no. 2, pp. 2225-2236, Jun. 2020.

[4] NOKIA, "Nokia to lead KOMSENS-6G, integrating sensing into the communications system," *Technical Report*, Nov. 2022, Available. [Online]: https://shorturl.at/MUY27.

[5] SAMSUNG, "Joint communication and sensing in 6G networks," *Technical Report*, Oct. 2021, Available. [Online]: https://shorturl.at/hAHKL.

[6] HUAWEI, "Integrated sensing and communication (ISAC)—From concept to practice," *Technical Report*, Sep. 2022, Available. [Online]: https://shorturl.at/bhS37.

[7] B. Chalise, M. Amin, and B. Himed, "Performance tradeoff in a unified passive radar and communications system," *IEEE Signal Process. Lett.*, vol. 24, no. 9, pp. 1275-1279, Sep. 2017.

[8] C.-C. Ouyang, Y. Liu, and H. Yang, "Fundamental performance of integrated sensing and communications (ISAC) systems," *arXiv Preprint*, 2022, Online. [Available]: https://arxiv.org/abs/2202.06207.

[9] C.-C. Ouyang, Y. Liu, and H. Yang, "On the performance of uplink ISAC systems," *arXiv Preprint*, 2022, Online. [Available]: https://arxiv.org/abs/2201.01422.

[10] Z. Xiao and Y. Zeng, "Full-duplex integrated sensing and communication: Waveform design and performance analysis," *2021 13th Int. Con. Wireless Commun. Signal Process. (WCSP)*, Changsha, China, 2021, pp. 1-5, doi: 10.1109/WCSP52459.2021.9613663.

[11] Z. Xiao and Y. Zeng, "Waveform design and performance analysis for full-duplex integrated sensing and communication," *IEEE J. Sel. Areas Commun.*, Early access, 2022, doi: 10.1109/JSAC.2022.3155509.

[12] M. Al-Jarrah, R. Al-Jarrah, N. Al-Ababneh, "Decision fusion in mobile wireless sensor networks using cooperative multiple symbol differential space time coding", *AEU-Int. J. Electron. Commun*., vol. 80, pp. 127-136, 2017.

[13] M. Al-Jarrah, E. Alsusa and C. Masouros, "Kullback-Leibler Divergence analysis for integrated radar and communications (RadCom)," *2023 IEEE Wireless Commun. Netw. Conf. (WCNC)*, Glasgow, United Kingdom, 2023, pp. 1-6, doi: 10.1109/WCNC55385.2023.10118838.

[14] M. Al-Jarrah, E. Alsusa and C. Masouros, "A unified performance framework for integrated sensing-communications based on KL-divergence," *IEEE Trans. Wireless Commun.*, vol. 22, no. 12, pp. 9390-9411, Dec. 2023, doi: 10.1109/TWC.2023.3270390.

[15] Y. Kloob, M. Al-Jarrah, E. Alsusa and C. Masouros, "Novel KLD-based resource allocation for integrated sensing and communication," *IEEE Trans. Signal Process.*, accepted with major revision.

[16] N. Fatema, G. Hua, Y. Xiang, D. Peng, and I. Natgunanathan, "Massive MIMO linear precoding: A survey," *IEEE Sys. J.*, vol. 12, no. 4, pp. 3920-3931, Dec. 2018, doi: 10.1109/JSYST.2017.2776401.